

DEPTH OF FORMATION OF SUPER-DEEP DIAMONDS

CHIARA ANZOLINI

Dipartimento di Geoscienze, Università di Padova, Via G. Gradenigo 6, 35131 Padova

Current address: Department of Earth and Atmospheric Sciences, University of Alberta, 1-26 Earth Sciences Building, Edmonton, Alberta T6G 2E3, Canada

INTRODUCTION

Diamonds, and the mineral inclusions they trap during growth, are pristine samples from the mantle that reveal processes operating in otherwise inaccessible regions of the Earth. This information is particularly valuable if it can be combined with depth estimates. The majority of diamonds are lithospheric, whilst the depth of origin of super-deep diamonds, which represent only 6% of the total (Stachel & Harris, 2008), is uncertain. Super-deep diamonds are considered to be sub-lithospheric, with formation from 300 to 800 km depth (Harte, 2010), on the basis of the inclusions trapped within them, which are believed to be the products of retrograde transformation from lower-mantle or transition-zone precursors (Fig. 1). However, in many cases undisputed evidence of these purported high-pressure precursors as inclusions in diamonds is lacking, and, consequently, their real depth of origin has been proven only in a few cases (e.g., Brenker *et al.*, 2002; Pearson *et al.*, 2014; Smith *et al.*, 2016; Nestola *et al.*, 2018).

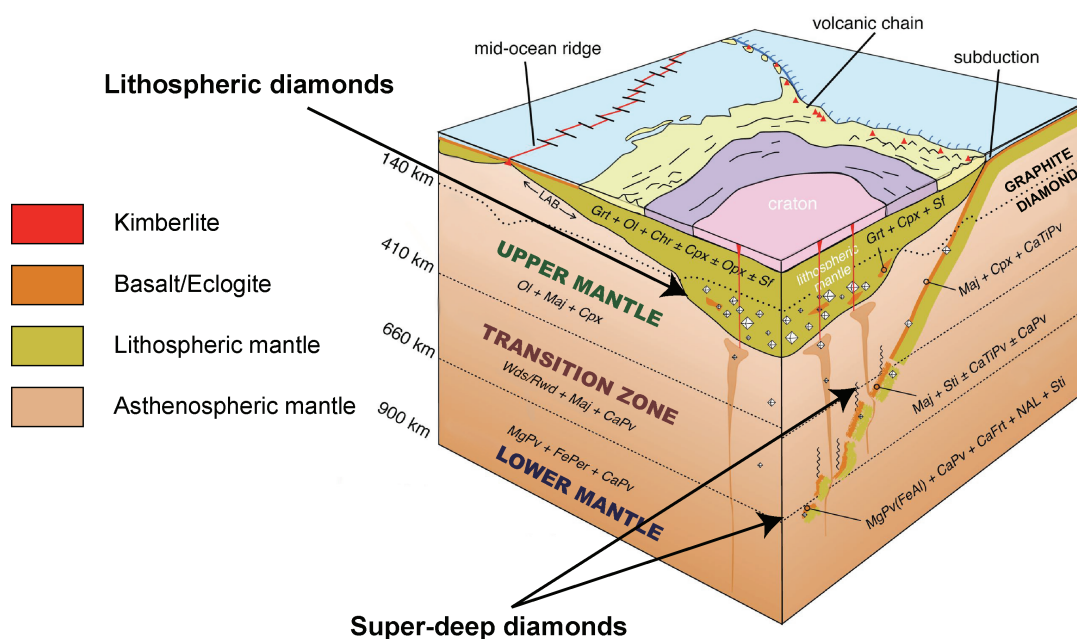


Fig. 1 - Block diagram showing the basic relationship between a continental craton, its lithospheric mantle keel and diamond stable regions in the keel, and the asthenospheric mantle. The upper mantle extends to 410 km, the transition zone is taken between the major seismic discontinuities at 410 km and 660 km depth, the lower mantle starts at 660 km (modified from Shirey *et al.*, 2013).

This Ph.D. thesis aimed to obtain the real depth of formation of super-deep diamonds by studying the most common mineral phases enclosed within them by non-destructive methods. We have studied about 40 diamonds with inclusion of CaSiO_3 -walstromite or ferropericlase using in-house single-crystal X-Ray Diffraction and micro-Raman spectroscopy as well as Field Emission Gun-Scanning Electron Microscopy, Synchrotron X-ray Tomographic Microscopy and Synchrotron Mössbauer source at outside Institutions. In

addition, laser-heating diamond-anvil cell experiments were performed on a synthetic Ti-free jeffbenite to determine if the absence of Ti extends the stability field of such mineral compared to previous studies. Finally, elastic geobarometry (Angel *et al.*, 2014a, b, 2015a, b, 2017), which is a non-destructive alternative to chemical geobarometry, based solely on the thermoelastic parameters of host and inclusion and on the residual pressure retained by the inclusion within the host, has been completed both on ferropericlaise and CaSiO₃-walstromite, in this last case together with thermodynamic and first-principles calculations.

One of our principal results suggests that CaSiO₃-walstromite may be considered a sub-lithospheric mineral, but retrograde transformation from a CaSiO₃-perovskite precursor is only possible if the diamond around the inclusion expands in volume by ~30%. Moreover, high-pressure and high-temperature experiments indicate that Ti-free jeffbenite, a new tetragonal phase with garnet-like stoichiometry (Nestola *et al.*, 2016b) previously referred to as TAPP (Tetragonal Almandine-Pyrope Phase), could be directly incorporated into diamond in the transition zone or uppermost lower mantle and therefore this mineral may represent a high-pressure marker to detect super-deep diamonds. Finally, the observation of magnesioferrite exsolutions within ferropericlaise, combined with elastic geobarometry results, strengthen the hypothesis that single ferropericlaise inclusions might not be reliable markers for a diamond lower-mantle provenance.

MATERIAL AND METHODS

The diamonds from São Luiz, Juina, Brazil, involved in this work are 2-8 mm in size and colourless to brown (Fig. 2). Recognized shapes include octahedra, dodecahedra and octahedra-dodecahedra transition forms, macles (twinned diamonds), and flattish irregular stones. Most of the diamonds are broken and heavily resorbed. Several samples show signs of plastic deformation and sometimes exhibit internal fractures at the diamond-inclusion interfaces.

Single-Crystal X-Ray Diffraction (Department of Geosciences, University of Padova)

X-ray data were collected using a Rigaku Oxford Diffraction SuperNova single-crystal diffractometer, equipped with a Dectris Pilatus 200 K area detector and with a Mova X-ray microsource. A monochromatized MoK α radiation ($\lambda = 0.71073 \text{ \AA}$), working at 50 kV and 0.8 mA, was used to minimize the absorption effects due to the large size of the host diamond. The sample-to-detector distance was 68 mm. Data reduction was performed using the CrysAlisPro software (Rigaku Oxford Diffraction) using frame scaling based on maximizing the agreement between intensities of symmetry-equivalent reflections.

Micro-Raman spectroscopy (Department of Geosciences, University of Padova)

Unless otherwise specified, Raman measurements were carried out with a Thermo ScientificTM DXR Raman Microscope using a 532 nm laser. The analyses were performed using a 50 \times objective with ~2.5 cm⁻¹ spectral resolution and 1.1 μm spatial resolution at 10 mW of power. Spectra were recorded in the frequency range extending from 100 to 3500 cm⁻¹. To maximize the signal-to-noise ratio, each spectrum was collected four times using an exposure time of 30 s, and then merged together at the end of the acquisition. Spectral fitting was carried out using the Thermo ScientificTM OMNICTM Spectra Software. The instrument was calibrated by using the calibration tool provided by Thermo ScientificTM.

Laser-heating diamond-anvil cell (School of Earth Sciences, University of Bristol)

Double-sided laser heating, where 100 W fiber lasers produced heated spots that were 20-30 μm in diameter, was performed in symmetric diamond-anvil cells with culet sizes of 250 μm . Re gaskets were pre-indented to a thickness of ~50 μm . In the first set of experiments the glass sample discs were loaded in between SiO₂ insulators into 90 μm diameter laser-drilled sample chambers. In a second set of experiment, the powdered-glass starting material (mixed with 10 wt.% Pt black as a laser absorber) was loaded into four 30 μm chambers laser-drilled in the indentation; no insulating material was used. In both cases the pressure was measured from the Raman shift of the singlet peak of the diamond culet.

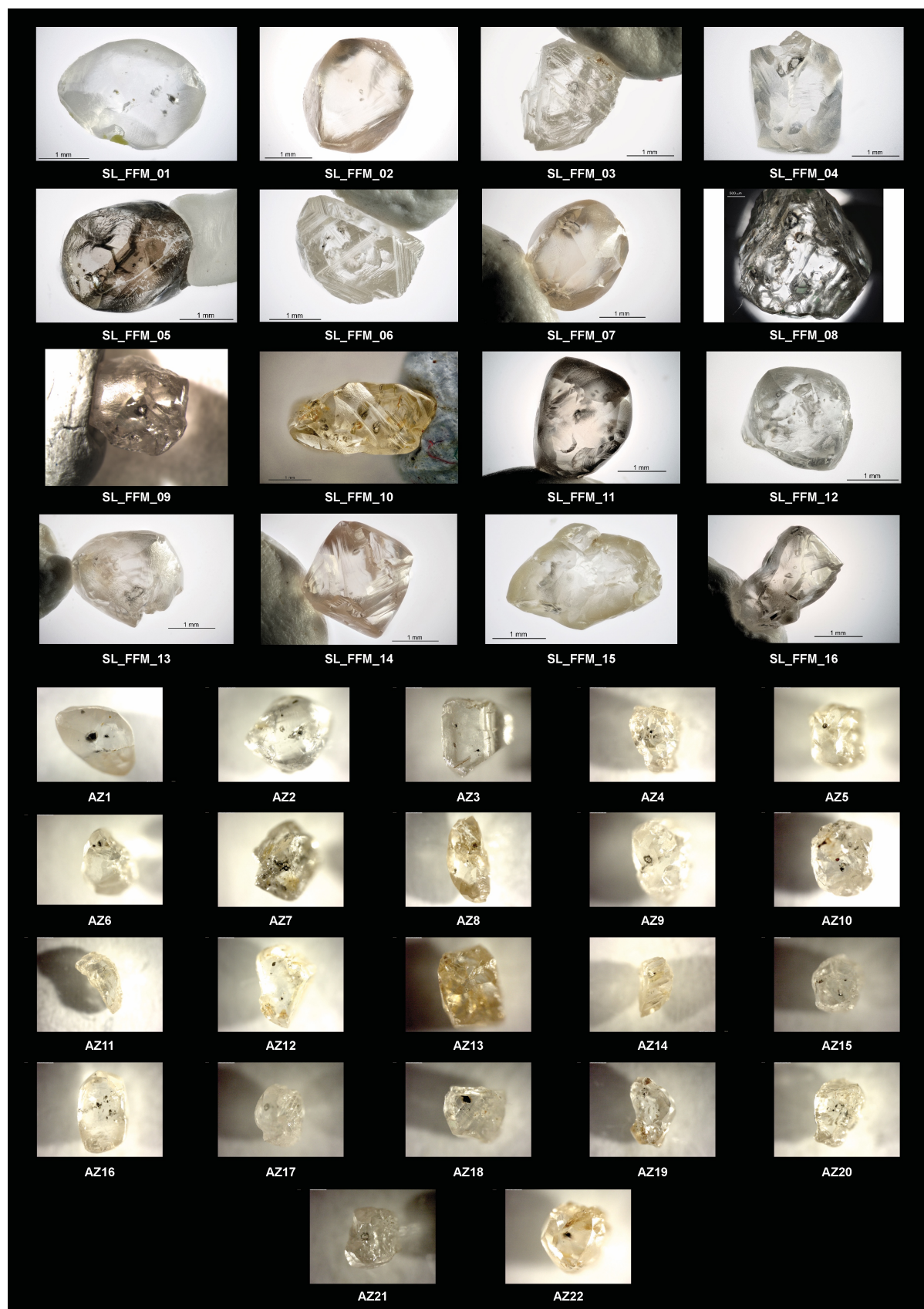


Fig. 2 - The diamonds from São Luiz, Juina, Brazil, studied in this work. Adapted from Anzolini (2018).

High-pressure micro-Raman spectroscopy (Department of Sciences, University of Roma Tre)

The Raman spectra were collected with a Horiba LabRam HR micro-Raman spectrometer equipped with a green solid-state laser (532 nm) focused through a 20× LWD objective. The spatial resolution of the sample surface was ~1 μm and the spectral resolution was 0.3 cm⁻¹. For the ruby, optical filters were employed in order to achieve ~1 mW at the sample surface; the Raman system was set with 1800 T grating, exposure time 1 s (3 times), confocal hole of 300 μm and slit of 200 μm. For the CaSiO₃-walstromite, optical filters were employed in order to achieve ~50 mW at the sample surface; the Raman system was set with 1800 T grating, exposure time 60 s (3 times), confocal hole of 100 μm and slit of 100 μm. For the high-pressure measurements a ETH DAC with 600 μm size culets was loaded with the crystal of CaSiO₃-walstromite, a piece of ruby as internal pressure standard and a 4:1 mixture of methanol:ethanol as pressure-transmitting medium. The calibration was done using the main Raman line (520.5 cm⁻¹) of a silicon standard.

Field Emission Gun - Scanning Electron Microscopy (Department of Physics and Astronomy, University of Padova)

Field Emission Gun–Scanning Electron Microscopy measurements were carried out using a Zeiss SIGMA HD FEG-SEM microscope operating at 20 kV, with a spot-size of ~1 nm. Imaging was performed using an InLens secondary electron detector. Compositional analysis was performed using an energy dispersive X-ray spectrometer (EDX by Oxford Instruments). The spatial resolution in microanalysis was of ~1 μm.

Synchrotron X-ray Tomographic Microscopy (Swiss Light Source, TOMographic Microscopy and Coherent rAdiology experimenTs beamline, Paul Scherrer Institute, Switzerland)

Measurements were performed at 60 KeV in order to reduce the X-ray absorption effects from the diamonds. The technique is based on the acquisition of a very large number of X-ray radiographs from different angular positions around a vertical rotation axis, followed by the application of a mathematical algorithm for the reconstruction of cross-sectional slices. Such slices can be stacked together to obtain a digital 3-D model of the investigated object.

Synchrotron Mössbauer Source (Nuclear Resonance beamline ID18, European Synchrotron Radiation Facility, Grenoble, France)

The narrow (~6 neV) energy component of X-rays at the Mössbauer energy of 14.4 keV was extracted from a wide spectrum of synchrotron radiation using a ⁵⁷FeBO₃ single-crystal monochromator and focused to a beam width of size of 10×15 μm² using Kirkpatrick- Baez mirrors. Each SMS spectrum took approximately 2 h to collect. The velocity scales of all Mössbauer spectra were calibrated relative to 25 mm thick α-Fe foil, and all spectra were fitted using the software package MossA.

Synchrotron powder X-ray diffraction (Beamline I15, Diamond Light Source, Rutherford Appleton Laboratory, United Kingdom)

The monochromatic X-ray beam had a diameter of ~6 μm and a wavelength of 0.4133 Å. The acquisition time was typically 10 s and the sample-to-detector distance was calibrated using a CeO₂ standard. Diffraction patterns were preliminarily integrated into 1-D spectra using the program Dioptas (Prescher & Prakapenka, 2015) and then fitted and indexed with the software HighScore Plus (PANalytical).

RESULTS AND DISCUSSIONS

During the first year we investigated several single phases and assemblages of Ca-silicate inclusions still trapped in a diamond by *in-situ* single-crystal X-ray diffraction and micro-Raman spectroscopy and we obtained a minimum entrapment pressure of ~5.7 GPa (~180 km) at 1500 K (Fig. 3). However, the observed coexistence of CaSiO₃-walstromite, larnite (β-Ca₂SiO₄) and CaSi₂O₅-titanite in one multiphase inclusion within the same diamond indicates that the sample investigated is sub-lithospheric with entrapment pressure between ~9.5 and

~11.5 GPa at 1500 K, based on experimentally-determined phase equilibria (Brenker *et al.*, 2005; Anzolini *et al.*, 2016). In addition, thermodynamic calculations suggested that, within a diamond, single inclusions of CaSiO₃-walstromite cannot derive from CaSiO₃-perovskite, unless the diamond expands by ~30% in volume (Anzolini *et al.*, 2016), but typical volume changes for diamonds by cooling and decompression are of the order of 1-3%, depending on the exact path.

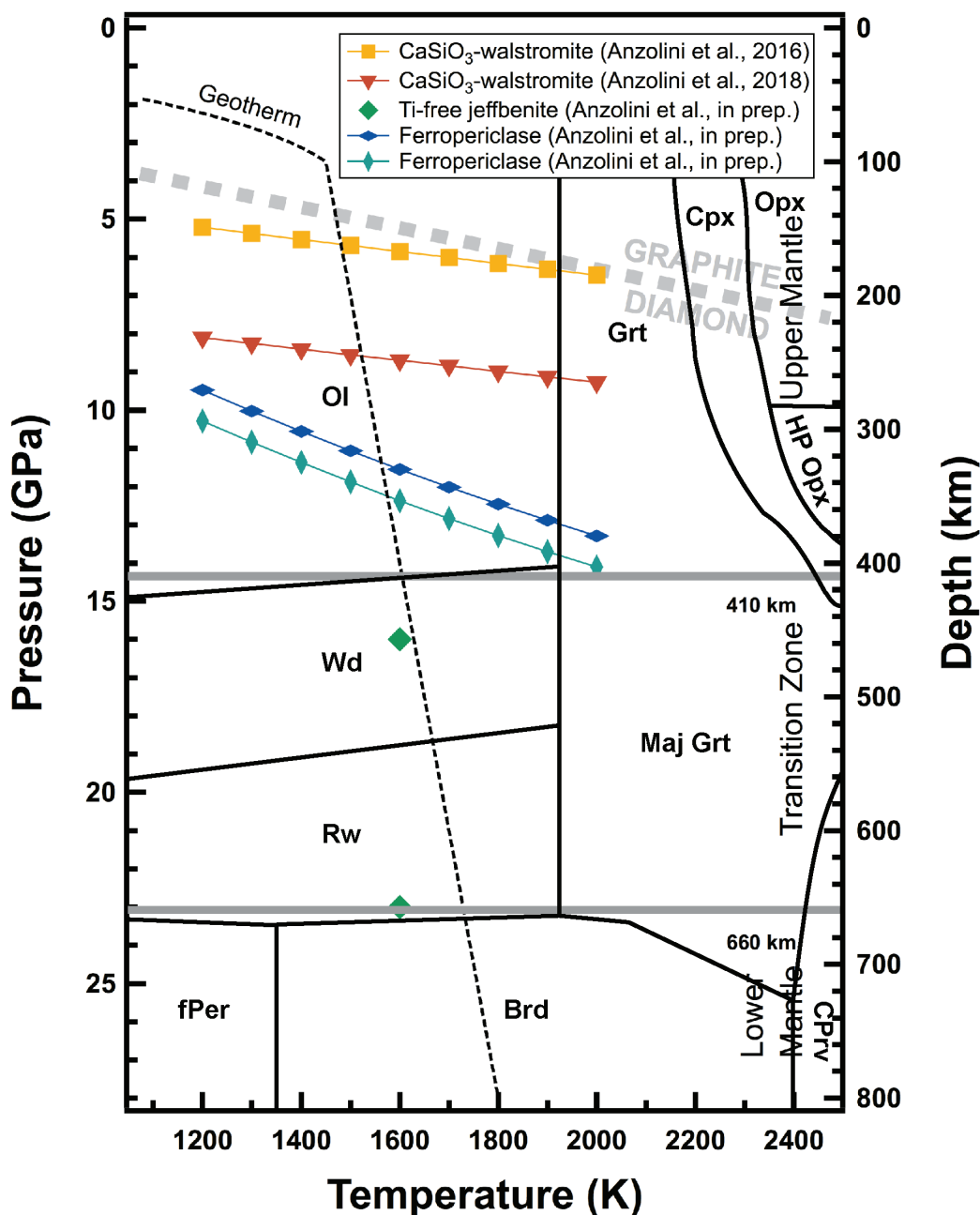


Fig. 3 - Phase diagram in which the phase boundaries are given as solid lines (Stixrude & Lithgow-Bertelloni, 2005). The graphite-diamond phase boundary is shown as a grey stippled line (Day, 2012). The geotherm is shown as a black dashed line (Turcotte & Schubert, 2014). The 410 and 660 km discontinuities enclosing the transition zone are indicated by bold lines. Adapted from Anzolini (2018).

During the second year we provided the first calibration curve to determine the residual pressure of a CaSiO_3 -walstromite inclusion by means of Raman spectroscopy without breaking the diamond. To do so, we performed high-pressure micro-Raman investigations on a CaSiO_3 -walstromite crystal under hydrostatic stress conditions within a diamond-anvil cell. We also calculated at different pressures the Raman spectrum of CaSiO_3 -walstromite by *ab initio* methods both under hydrostatic and non-hydrostatic stress conditions to avoid misinterpretation of the results caused by the possible presence of deviatoric stresses causing anomalous shift of CaSiO_3 -walstromite Raman peaks. Finally, we applied elastic geobarometry to estimate the minimum entrapment pressure of a CaSiO_3 -walstromite inclusion trapped in a natural diamond, which resulted to be ~ 9 GPa (~ 260 km) at 1800 K (Fig. 3). These results indicated that the diamond investigated was certainly sub-lithospheric (Anzolini *et al.*, 2018).

In addition, we performed laser heated diamond-anvil cell experiments on a synthetic Ti-free jeffbenite, in order to determine the role that TiO_2 plays in its stability field and to determine if this mineral could be directly incorporated into diamond in the deep transition zone or lower mantle. With respect to previous studies (Armstrong & Walter, 2012), our results indicated that the absence of TiO_2 extends the stability field of jeffbenite to ~ 23 GPa (~ 660 km) at 1600 K (Fig. 3), demonstrating that Ti-free jeffbenite may represent one of the most reliable markers for diamonds super-deep origin (Anzolini, 2018).

During the third year we studied two ferropericlases, extracted from a single diamond, by Synchrotron X-ray Tomographic Microscopy (SXRTM), Synchrotron Mössbauer Source (SMS; Nestola *et al.*, 2016a), Single-Crystal X-ray Diffraction (SCXRD) and Field Emission Gun–Scanning Electron Microscopy (FEG-SEM). SXRTM did not show any fractures around the ferropericlase inclusions. Both SCXRD and FEG-SEM showed nanometer-sized exsolutions of magnesioferrite within the inclusions. We also completed elastic geobarometry, which provided an estimate for the depth of entrapment of the two ferropericlase - diamond pairs and placed their origin between the upper mantle and the transition zone, at ~ 12 GPa (~ 340 km) at 1500 K (Fig. 3). These results strengthened the hypothesis that single ferropericlase inclusions might not be reliable markers for a lower-mantle provenance of super-deep diamonds, although their presence indicates a sub-lithospheric origin (Anzolini, 2018).

CONCLUSIONS

The concluding remarks can be summarized as follows:

- i) Single CaSiO_3 -walstromite and ferropericlase inclusions cannot currently suggest a lower-mantle origin for super-deep diamonds, although their presence indicates a sub-lithospheric origin;
- ii) Ti-free jeffbenite and ringwoodite inclusions are, at the moment, the only examples of mineral phases found within diamonds which unambiguously indicate a diamond origin down to ~ 660 km depth;
- iii) Elastic geobarometry, being based upon several assumptions, is often able to provide only a minimum estimate for the depth of entrapment of an inclusion within its host. However, the possibility of being applied to any diamond-inclusion couple, allowed us to confirm that super-deep diamonds, in the specific sense of sub-lithospheric, definitely exist.

ACKNOWLEDGMENTS

This Ph.D. project was financially supported by Fondazione Cassa di Risparmio di Padova e Rovigo and project “INclusions in Diamonds: MEssengers from the Deep EArth”, funded by the ERC Starting Grant 2012 to Fabrizio Nestola (N° 307322). The DeBeers Group of Companies is thanked for the donation of the diamonds to Jeffrey W. Harris.

REFERENCES

- Angel, R.J., Alvaro, M., Gonzalez-Platas, J. (2014a): EosFit7c and a fortran module (library) for equation of state calculations. *Z. Krist.-Cryst. Mater.*, **229**, 405-419.
- Angel, R.J., Mazzucchelli, M.L., Alvaro, M., Nimis, P., Nestola, F. (2014b): Geobarometry from host-inclusion systems: The role of elastic relaxation. *Am. Mineral.*, **99**, 2146-2149.
- Angel, R.J., Alvaro, M., Nestola, F., Mazzucchelli, M.L. (2015a): Diamond thermoelastic properties and implications for determining the pressure of formation of diamond-inclusion systems. *Russ. Geol. Geophys.*, **56**, 211-220.
- Angel, R.J., Nimis, P., Mazzucchelli, M.L., Alvaro, M., Nestola, F. (2015b): How large are departures from lithostatic pressure? Constraints from host-inclusion elasticity. *J. Metamorph. Geol.*, **33**, 801-813.
- Angel, R.J., Mazzucchelli, M.L., Alvaro, M., Nestola, F. (2017): EosFit-Pinc: A simple GUI for host-inclusion elastic thermobarometry. *Am. Mineral.*, **102**, 1957-1960.
- Anzolini, C. (2018): Depth of formation of super-deep diamonds. Tesi di Dottorato in Scienze della Terra, Università degli Studi di Padova, Padova, Italy, 190 p.
- Anzolini, C., Angel, R.J., Merlini, M., Derzsi, M., Tokár, K., Milani, S., Krebs, M.Y., Brenker, F.E., Nestola, F., Harris, J.W. (2016): Depth of formation of CaSiO₃-walsstromite included in super-deep diamonds. *Lithos*, **265**, 138-147.
- Anzolini, C., Prencipe, M., Alvaro, M., Romano, C., Vona, A., Lorenzon, S., Smith, E.M., Brenker, F.E., Nestola, F. (2018): Depth of formation of super-deep diamonds: Raman barometry of CaSiO₃-walsstromite inclusions. *Am. Mineral.*, **103**, 69-74.
- Armstrong, L.S. & Walter, M.J. (2012): Tetragonal almandine pyrope phase (TAPP): Retrograde Mg-perovskite from subducted oceanic crust? *Eur. J. Mineral.*, **24**, 587-597.
- Brenker, F.E., Stachel, T., Harris, J.W. (2002): Exhumation of lower mantle inclusions in diamond: ATEM investigation of retrograde phase transitions, reactions and exsolution. *Earth Planet. Sc. Lett.*, **198**, 1-9.
- Brenker, F.E., Vincze, L., Vekemans, B., Nasdala, L., Stachel, T., Vollmer, C., Kersten, M., Somogyi, A., Adams, F., Joswig, W. (2005): Detection of a Ca-rich lithology in the Earth's deep (> 300 km) convecting mantle. *Earth Planet. Sc. Lett.*, **236**, 579-587.
- Day, H.W. (2012): A revised diamond-graphite transition curve. *Am. Mineral.*, **97**, 52-62.
- Harte, B. (2010): Diamond formation in the deep mantle: The record of mineral inclusions and their distribution in relation to mantle dehydration zones. *Mineral. Mag.*, **74**, 189-215.
- Nestola, F., Cerantola, V., Milani, S., Anzolini, C., McCammon, C., Novella, D., Kuppenko, I., Chumakov, A., Rüffer, R., Harris, J.W. (2016a): Synchrotron Mössbauer Source technique for *in situ* measurement of iron-bearing inclusions in natural diamonds. *Lithos*, **265**, 328-333.
- Nestola, F., Burnham, A.D., Peruzzo, L., Tauro, L., Alvaro, M., Walter, M.J., Gunter, M., Anzolini, C., Kohn, S.C. (2016b): Tetragonal Almandine-Pyrope Phase, TAPP: finally a name for it, the new mineral jeffbenite. *Mineral. Mag.*, **80**, 1219-1232.
- Nestola, F., Korolev, N., Kopylova, M., Rotiroti, N., Pearson, D.G., Pamato, M.G., Alvaro, M., Peruzzo, L., Gurney, J.J., Moore, A.E., Davidson, J. (2018): CaSiO₃-perovskite in diamond indicates the recycling of oceanic crust into the lower mantle. *Nature*, **555**, 237-241.
- Pearson, D.G., Brenker, F.E., Nestola, F., McNeill, J., Nasdala, L., Hutchison, M.T., Matveev, S., Mather, K., Silversmit, G., Schmitz, S. (2014): Hydrous mantle transition zone indicated by ringwoodite included within diamond. *Nature*, **507**, 221-224.
- Prescher, C. & Prakapenka, V.B. (2015): DIOPTAS: A program for reduction of two-dimensional X-ray diffraction data and data exploration. *High Pressure Res.*, **35**, 223-230.
- Shirey, S.B., Cartigny, P., Frost, D.J., Keshav, S., Nestola, F., Nimis, P., Pearson, D.G., Sobolev, N.V., Walter, M.J. (2013): Diamonds and the geology of mantle carbon. *Rev. Mineral. Geochem.*, **75**, 355-421.
- Smith, E.M., Shirey, S.B., Nestola, F., Bullock, E.S., Wang, J., Richardson, S.H., Wang, W. (2016): Large gem diamonds from metallic liquid in Earth's deep mantle. *Science*, **354**, 1403-1405.
- Stachel, T. & Harris, J.W. (2008): The origin of cratonic diamonds-constraints from mineral inclusions. *Ore Geol. Rev.*, **34**, 5-32.
- Stixrude, L. & Lithgow-Bertelloni, C. (2005): Thermodynamics of mantle minerals-I. Physical properties. *Geophys. J. Int.*, **162**, 610-632.
- Turcotte, D. & Schubert, G. (2014): Geodynamics (3rd ed.). Cambridge University Press, 636 p.